Geochemistry Geophysics Geosystems G3
AN ELECTRONIC JOURNAL OF THE EARTH SCIENCES
PUBLISHED BY AGU AND THE GEOCHEMICAL SOCIETY

Article
Volume 1
December 13, 1999
Paper Number 1999GC000011
ISSN: 1525-2027

Crustal Motion North and South of the Arica Deflection: Comparing Recent Geodetic Results from the Central Andes

Michael Bevis *(bevis@soest.hawaii.edu)* and Eric C. Kendrick
Hawaii Institute of Geophysics and Planetology, University of Hawaii

Robert Smalley Jr.
Center for Earthquake Research and Information, University of Memphis

Thomas Herring
Department of Earth, Atmospheric and Planetary Sciences, MIT

Jorge Godoy
Instituto Geográfico Militar de Chile

Fernando Galban
Instituto Geográfico Militar de Argentina, Buenos Aires, Argentina

Abstract. **[1]** An intercomparison of recent velocity solutions for the Global Positioning System (GPS) networks constructed by the South America–Nazca Plate Project (SNAPP), based in Bolivia and Peru, and our Central Andes GPS Project (CAP), based in Chile and Argentina, indicates a velocity discontinuity of order 10 mm/yr near the boundary between these networks. We suggest that this velocity jump manifests measurement bias in the SNAPP velocity field. Our results indicate that no major slip partitioning occurs within the forearc of northern Chile in response to the obliquity of subduction but that Nazca–South America plate convergence is partitioned between the forearc and the backarc regions. The present rate of shortening across the southern part of the Sub-Andean belt in Argentina is 8.9 ± 1.6 mm/yr.

Keywords: Central Andes; GPS geodesy; crustal motion; reference frames.
Index terms: Crustal movements–interplate; GPS geodesy; crustal motion; reference frames.
Received August 26, 1999; **Accepted** November 5, 1999; **Published** December 13, 1999
Bevis, M., et al., 1999. Crustal motion north and south of the Arica deflection: Comparing recent geodetic results from the central Andes, *Geochem. Geophys. Geosyst.*, vol. 1, Paper number 1999GC000011 [5881 words, 4 figures, 2 tables]. Dec. 13, 1999.

1. Introduction

[2] One of the major themes of the burgeoning literature on the geology and geodynamics of the Central Andes is the importance of along-strike variability and segmentation within this broad plate boundary zone [*Jordan et al.*, 1983]. Quantities that vary along the strike of the orogen include the obliquity of plate convergence [*McCaffrey*, 1994], the dip of the subducting plate [*Barazangi and Isacks*, 1976; *Bevis and Isacks*, 1984; *Cahill and Isacks*, 1993], the presence or absence of an active volcanic arc [*Barazangi and Isacks*, 1976; *Nur and Ben Avraham*, 1981], the width and height of the mountain belt [*Isacks*, 1988], its crustal thickness [*Allmendinger et al.*, 1997], and the tectonic style of foreland shortening [*Jordan et al.*, 1983]. Several segment boundaries are associated with bathymetric ridges and fracture zones impinging on the trench [*Nur and Ben Avraham*, 1981; *Pilger*, 1981; *Bevis and Isacks*, 1984; *Von Huene et al.*, 1997].

[3] Perhaps the most impressive changes along the strike of this margin occur in the vicinity of the Arica deflection and the nearby termination of the Altiplano-Puna physiographic province (Figure 1). Paleomagnetic studies indicate rotation of the forearc and the mountain belt relative to the craton, with anticlockwise rotation dominating in the northern limb of the Bolivian Orocline and clockwise rotation dominating in its southern limb [*Isacks*, 1988; *Randall*, 1998; *Beck*, 1998]. *Isacks* [1988] suggested that this pattern of rotation manifests along-strike variation in the magnitude of Cenozoic crustal shortening across the central Andes, but many paleomagnetic specialists explain the same observations in terms of local block rotations or a combination of local crustal rotation and the regional pattern of rotation invoked by *Isacks* [1988]. *Beck* [1988] argued that local block rotations are driven by distributed margin-parallel shear resulting from oblique subduction. While there is a very pronounced change in the obliquity of subduction near the Arica deflection [*McCaffrey*, 1994], the tectonic framework is further complicated by subduction of the Nazca Ridge and by nearby changes in the dip of the subducting slab (Figure 1 and Figure 2). This is one of the sharpest changes in slab dip observed at intermediate depths anywhere on Earth [*Bevis and Isacks*, 1984].

[4] Several crustal motion projects utilizing Global Positioning Systems (GPS) geodesy are underway in the Central Andes. *Norabuena et al.*, [1998] recently presented crustal velocity estimates for the SNAPP network located in Peru and Bolivia. The results from their GPS network (Figures 2 and 3) suggest that trench-parallel velocity gradients are important. For example, the velocity vectors for stations TANA, COTA and the six stations northwest of TANA and COTA all bear E (except one that bears ESE), while almost every other vector in the coastal zone and in the high mountains bears ENE (Figure 2). Note how these two groups of stations are positioned relative to the flat part of the slab. The larger margin-parallel component of velocity for stations in the flat slab segment of the margin is not easily explained in terms of strain partitioning driven by the obliquity of subduction, since obliquity is of similar and sometimes greater magnitude in the adjacent steep slab segment of the plate boundary but SNAPP's velocity solutions there have smaller margin-parallel components (Figure 2).

[5] The Central Andes GPS Project (CAP) has been operating in Chile and Argentina since 1993. We recently presented a geodetic analysis of a sparse continental-scale network of continuous GPS (or CGPS) stations that we use as a regional spatial reference system, following the strategy described by *Bevis et al.* [1997]. In this paper we present the results we have obtained using roving GPS measurements in northern Chile and Argentina, and compare them with those obtained further north and west by *Norabuena et al.* [1998]. An immediate objective is to clarify the geodetic problem identified by *Kendrick et al.* [1999], a serious disagreement on the velocity estimated by *Norabuena et al.* [1998] and by us for the IGS station AREQ (Arequipa). This is an important technical issue since AREQ is the only CGPS station within the SNAPP network. The suggestion is that although both groups are nominally working in craton-fixed frames, our frames may not, in fact, be equivalent.

2. Data Analysis and Selection

[6] Our GPS data analysis procedures were described by Kendrick et al. (1999) and this information will not be repeated here. We have analyzed GPS observations obtained from 16 CGPS stations within South America from early 1993 (we have constructed eight of these stations since late 1995) and more than 100 rover GPS stations located in Chile and Argentina. These rover stations were observed in a series of field campaigns, the first of which was mounted in 1993. We present station velocities in a reference frame that nominally fixes the stable core or craton of the South American plate. In this frame the RMS horizontal velocity of the eight

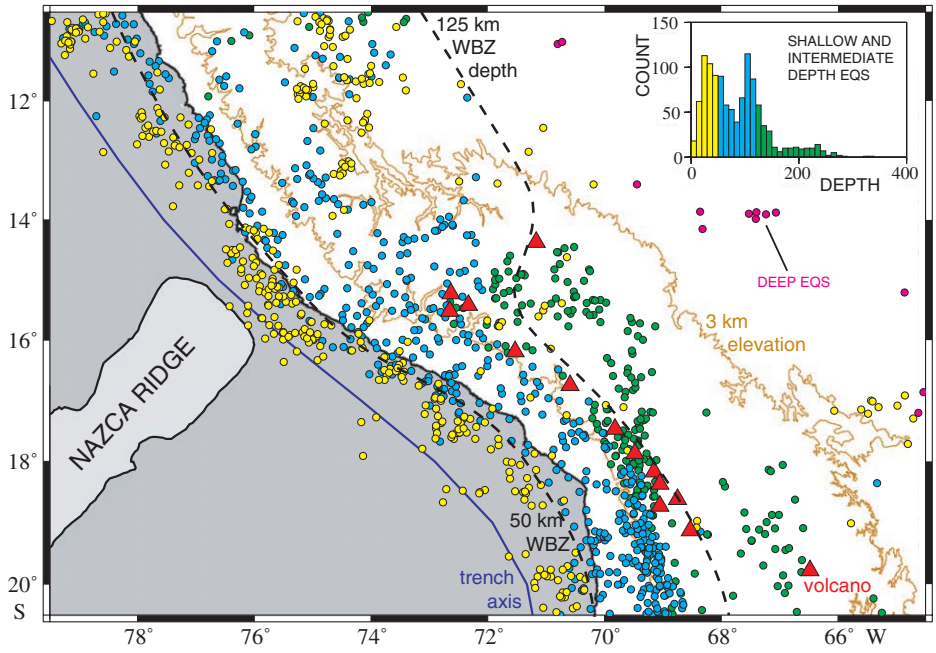

Figure 1. *Seismicity, active volcanism and topography near the Arica deflection. Well-located hypocenters from relocation of International Seismological Centre (ISC) and National Earthquake Information Center (NEIC) arrival time data* [Engdahl et al., 1998] *for the time period (1964–1995) are color-coded according to focal depth (0–50 km yellow, 50–120 km blue, 120–400 km green, deeper than 400-km magenta). The distribution of focal depths for all shallow and intermediate depth earthquakes (EQS) is shown in the inset histogram. Also shown are the* Cahill and Isacks [1993] *50- and 125-km isodepth contours for the middle of the Wadati-Benioff Zone (WBZ). Note the sharp change in the dip of the subducting slab and the spatially coincident terminus of the active volcanic arc. The 3-km elevation contour clearly indicates the nearby termination of the wide Altiplano-Puna physiographic province. The change from a narrow and linear mountain belt in the northwest to the wider and more strongly curved topography of the central Andes occurs close to the projection of the southeast flank of the Nazca Ridge. This feature is subducting with the Nazca plate, and consequently, its zone of intersection with the plate boundary is migrating southeastward along the trench.*

CGPS stations located within the craton is just 1.3 mm/yr. In contrast, our coastal CGPS station IQQE (Iquique) in northern Chile, for example, has a velocity of 24.5 ± 0.4 mm/yr, N77° ± 1°E. (All uncertainties stated in the text of this paper are one sigma standard errors.) Some CAP velocity solutions presented here differ very slightly from those given by *Kendrick et al.* [1999] since our latest geodetic analysis includes several months of additional CGPS data.

[7] In estimating formal uncertainties or standard errors for our velocity solutions, we attempt to account for the "colored noise" problem (i.e., temporal correlations in our positioning errors) following the analysis of *Zhang et al.* [1997]. Data decimation tests and (in the case of CGPS stations) time series truncation tests indicate that our error estimates are fairly reasonable [*Kendrick et al.*, 1999]. Nevertheless, neither we nor anyone known to us claims to understand the specific mechanism or mechanisms responsible for temporally correlated positioning noise. In practice, it can be suprisingly difficult to estimate the parameters of a known (i.e., specified) stochastic process from a time series which is not much longer than any correlation time associated with the process [*Gelb*, 1974]. Today's GPS geodesist is in an even more tenuous situation in that he or she cannot be sure even of the class(es) of stochastic process that best represent daily position-

ing error. It is for this reason that we place importance on the fact that we have eight CGPS stations in the craton and that they have an RMS horizontal velocity of just 1.3 mm/yr in our craton-fixed frame. This provides us with an external basis for assessing the typical levels of error in our CGPS velocity solutions. Many of the CGPS sites are not built in rock, and so at least some of the residual motion manifests site instability. This suggests CGPS velocity error does not greatly exceed 1 mm/yr. It could be smaller than this depending on the typical level of nontectonic motion at these CGPS stations (another unknown). We suggest that someone seeking an alternate and defensive estimate of velocity error might add 1 mm/yr to all our nominal standard errors. As to the uncertainties that we assign to the velocities of our rover GPS stations, we believe that the spatial coherence of our velocity field indicates that our formal errors cannot be significantly underestimated.

[8] Our rover GPS stations in northern Chile and NW Argentina were first occupied in March 1993 and were reoccupied nearly 4 years later. The general pattern of the velocity field north of 35°S is fairly similar to that reported by *Norabuena et al.* [1998] and *Kendrick et al.* [1999], except in one important regard. Whereas the displacements at most of these stations manifest the interseismic velocity field, the motions of stations between ~22.5°S and 24°S are significantly affected by, and are often totally dominated by, the coseismic displacement field of the 1995 (M_s = 7.6) Antofagasta earthquake [*Klotz*

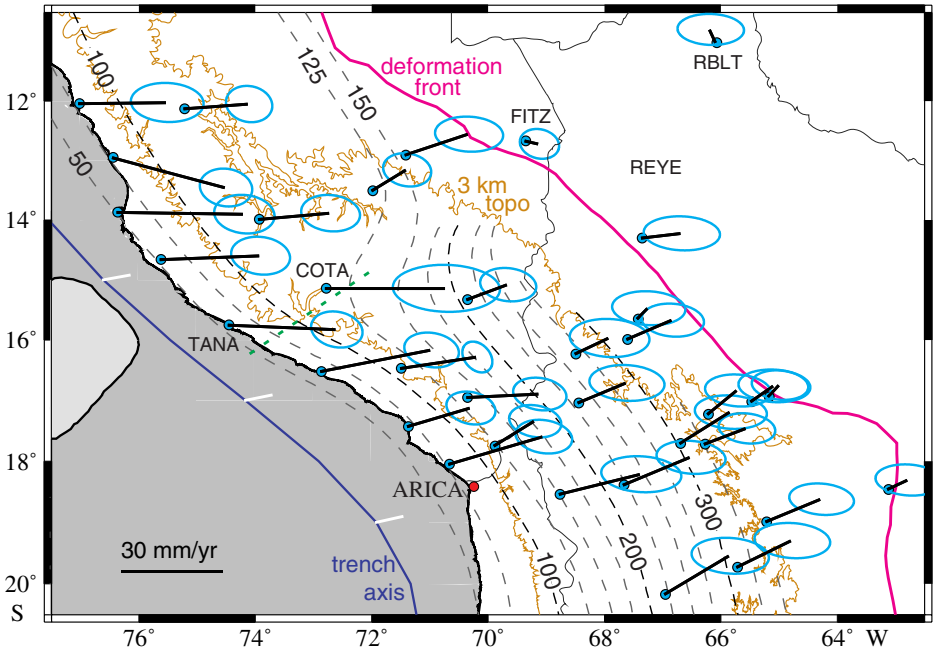

Figure 2. The interseismic velocity field estimated by SNAPP *[Norabuena et al., 1998]* for the central Andes and adjacent areas in Bolivia and Peru. The error ellipses are 95% confidence intervals. The dashed lines are the contours of *Cahill and Isacks [1992]* indicating depth (in km) to the middle of the Wadati-Benioff zone. Note the difference in the typical direction of the velocity vectors in the group of stations located northwest of the green dashed line (near stations COTA and TANA) versus the group of stations located southeast of this line. This line roughly corresponds to the famous flat slab–steep slab transition in southern Peru. The short white lines projecting from the trench axis indicate the direction (but not the magnitude) of Nazca–South America plate convergence according to NUVEL-1A. Note that the obliquity of plate convergence near the stations southeast of the green line is comparable to and locally greater than the obliquity near the stations located northwest of the green line. Accordingly, one cannot easily invoke the obliquity of plate convergence to explain the large margin-parallel component of velocity found at the stations located northwest of the green line. Stations FITZ, REYE, and RBLT are all located in the craton.

et al., 1996, 1999]. Accordingly, for the purposes of comparing our velocity solutions with those of Norabuena et al., [1998] we must restrict our attention to that portion of our network located north of ~22.5°S (Figure 3). We will present a velocity solution for the rest of our GPS network in a future and longer paper.

3. Comparison of Velocity Solutions

[9] We have plotted both our velocity solutions and those presented by Norabuena et al. [1998] in Figure 3. Norabuena et al. [1998] realized their nominally craton-fixed frame by minimizing the motion of four IGS stations (KOUR, FORT, BRAZ, and LPGS) located near the Atlantic margin of South America and two of their own rover stations located near the western edge of the craton. These local cratonic stations, RBLT and SJCH, are shown in Figures 2 and 3, respectively. Our solutions are referenced to a frame which nearly fixes eight widely spaced CGPS stations (the four IGS stations above plus LHCL, PARC, PARA, and UEPP). The only station located within the study area and incorporated in both analyses is the IGS station AREQ, which is the only CGPS station located within the SNAPP network. Whereas *Norabuena et al.* [1998] assign AREQ a velocity of 22.6 ± 1.7 mm/yr, we estimate a velocity of 10.9 ± 0.3 mm/yr. The vector difference is 12.1 mm/yr bearing nearly east. Our solution is compatible with those reported by *Angermann et al.* [1999] and *Leffler et al.* [1997], i.e., 11.8 ± 0.8 mm/yr and 13.3 ± 1.5 mm/yr, respectively.

[10] We need to extend our comparison beyond a single station. Our first approach is to compare solutions for nearly collocated pairs of stations. There are four pairs of CAP and SNAPP rover stations that are located in close or fairly close proximity: coastal stations ARIC and CMOR near the Peru-Chile border, pairs CHNG and SACA and SLAS and OLLA near the Bolivia–Peru border, and pair YAVI and TARI near the Bolivia–Argentina border (Figure 3). With the exception of the first pair (ARIC and CMOR) the SNAPP station is located cratonward of the CAP station, so we would expect the SNAPP station to be moving a little slower. As we see in Table 1, however, in every case the SNAPP station is moving faster, with the vector differences (SNAPP - CAP) falling in the range 5.2–11.5 mm/yr, N83°–112°E. The mean velocity difference for all comparisons in Table 1 (including that for AREQ) has north and east components of -0.8 ± 1.1 mm/yr and +8.9 ± 1.9 mm/yr, respectively. Since the SNAPP station was located farther "downstream" in the regional velocity field than was the CAP station for three of the five intercomparisons, the second quantity might be viewed as an estimated lower bound on the eastward component of velocity bias between the CAP and SNAPP solutions near the boundary between the networks.

[11] We can also compare the CAP and SNAPP velocity fields in an aggregate sense. We do this by constructing velocity profiles that characterize the systematic decline of GPS station velocities as the stations get farther from the trench axis and then compare the profiles rather than individual station pairs. We restrict this comparison to those stations located within the "steep slab" segment of the Nazca plate. In this area the mean direction of both the CAP and the SNAPP velocities lies close to N72°E. This is also the azimuth of the vertical plane of maximum topographical symmetry between the north and south limbs of the Bolivian Orocline (Figure 4a) [*Gephart*, 1994]. There is a less perfect but still striking mirror symmetry, relative to this same plane, in the morphology of the subducted Nazca slab [*Gephart*, 1994]. Accordingly, we choose to measure trench-station separation in the direction N72°E, and to project all velocities onto this direction for the purpose of constructing velocity profiles.

[12] We have classified all the GPS stations that lie over the steep slab segment of the orogen into three classes: (1) the CAP stations, (2) the SNAPP stations lying immediately "downstream" of the CAP stations, and (3) the SNAPP stations located elsewhere. These groups of stations are color-coded in map view in Figure 4a. The (ve-

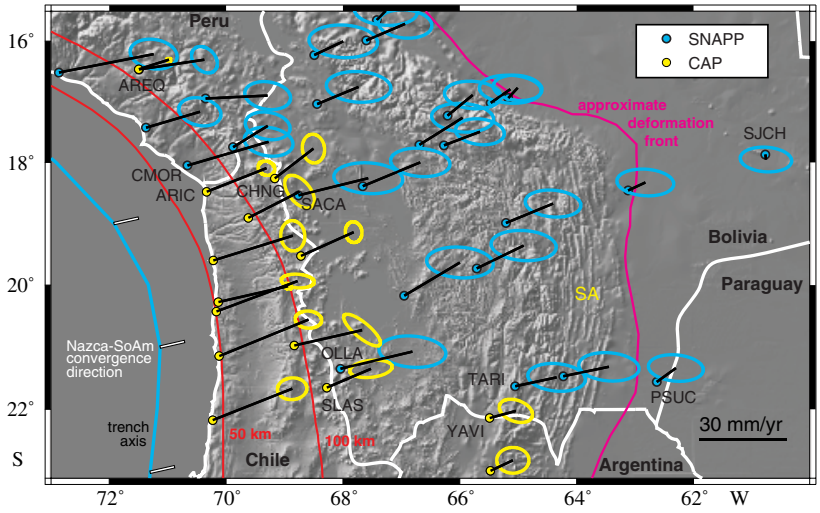

Figure 3. *Map showing CAP's and SNAPP's velocity solutions, both nominally presented in a craton-fixed frame. The SNAPP vectors, color-coded blue, are from Norabuena et al. [1998]. All error ellipses are 95% confidence intervals. The International GPS Service (IGS) station AREQ in Arequipa is the only station common to both groups that is located within the central Andes. The shaded relief map emphasizes short-wavelength topography. Note the parallel topographic ridges of the sub-Andean belt (marked SA). The thick magenta curve approximates the recent geological deformation front. Note that stations PSUC and SJCH are located within the craton. All stations with four-letter labels are referred to in the text. CAP station ARIC is located in the city of Arica. The two red curves are 50- and 100-km contours from* Cahill and Isacks [1992] *indicating depth to the middle of the Wadati-Benioff Zone (WBZ). The blue curve indicates the trench axis. The white lines originating from the trench axis are used to indicate the direction (not the magnitude) of the Nazca–South America plate convergence vector, as predicted by NUVEL-1A. While the coastline has an abrupt change in its orientation near Arica, the trench axis and the WBZ contours indicate that the orientation of the plate boundary changes much more gradually (also seen in* ***Figure 2****).*

locity weighted) mean azimuths of these groups are N69°E, N67°E, and N75°E, respectively. (The mean azimuth for both SNAPP groups combined is N71°E.) The corresponding velocity profiles are shown in Figure 4c. See the Figure 4 caption for additional details. Consider the profiles for the stations of group (1) in yellow and group (2) in blue. We would expect these profiles to coincide at trench–station distances near 300–330 km where these two groups of stations abut. Instead, the blue SNAPP profile appears to be displaced ~9–12 mm/yr up the velocity axis relative to the yellow CAP profile. This seems to confirm the velocity bias identified in Table 1.

[13] We suggest that Norabuena et al. [1998] have overestimated the velocity of all stations near the southwest limit of their network (Figure 3) by ~10 mm/yr. This local bias mostly affects the east component of SNAPP's velocity field (Table 1). The red SNAPP velocity profile better agrees with the yellow CAP profile than with the blue SNAPP profile (Figure 4c). This might reflect real along-strike variation in the velocity profile. Alternatively, the magnitude of the velocity bias might be varying in space. One might also invoke a combination of these explanations. It seems unlikely that we can resolve this issue until there are better ties between the CAP and SNAPP networks.

4. Velocity Biases and the Reference Frame

[14] It is probable that a large part of the bias between SNAPP's and CAP's velocity fields derives from reference frame problems. Specific reference frames are realized through the coordinates and velocities assigned to a set of sta-

tions. The greater the number of stations used to do this, and the more accurately the relative geometry of these stations is measured, the more consistent and stable the reference frame is. The error ellipses for SNAPP's rover GPS stations are significantly larger than those for CAP's rover stations. Probably most of this difference is due to CAP's total observational time span being roughly double that of SNAPP's. We find it more difficult to account for the difference between the uncertainties assigned to the CGPS stations. As mentioned above, we realized our cratonic reference frame by minimizing the horizontal motions of eight CGPS stations located in the stable core of the South American plate. The daily position time series at these eight stations had total time spans in the range 1.8 – 6.4 years, with the typical span being nearly 4 years. The residual horizontal velocities of these stations fall in the range 0.5 – 1.8 mm/yr, with an overall RMS value of just 1.3 mm/yr. SNAPP's cratonic reference frame was realized using just four CGPS stations and two rover stations. Their residual horizontal motions ranged between 1.1 and 7.1 mm/yr, with an RMS value of 4 mm/yr. The four CGPS stations have an RMS horizontal velocity of 4.3 mm/yr. The largest residual motion, 7.1 ± 3.5 mm/yr, occurs at IGS station LPGS near Buenos Aires in Argentina. The standard error assigned to this station is about half the magnitude of its residual motion. In this sense the motion is barely significant. On the other

Table1. Velocity Comparisons for Neighbouring Pairs of Stations from the CAP and SNAPP networks, and at the station AREQ which was incorporated into both networks.

Station	v_N	v_E	Solution
CMOR	8.1 ± 2.0	27.7 ± 3.4	SNAPP
ARIC	8.1 ± 1.0	20.4 ± 1.2	CAP
difference	0.0 ± 2.3	7.3 ± 3.6	
SACA	5.9 ± 2.2	23.9 ± 4.8	SNAPP
CHNG	10.2 ± 2.0	13.3 ± 1.6	CAP
difference	-4.3 ± 3.0	10.6 ± 5.1	
OLLA	5.9 ± 2.2	24.6 ± 4.7	SNAPP
SLAS	6.4 ± 1.2	15.1 ± 3.0	CAP
difference	-0.6 ± 2.5	9.5 ± 5.5	
TARI	3.0 ± 1.9	14.1 ± 4.0	SNAPP
YAVI	2.4 ± 1.6	9.0 ± 2.3	CAP
difference	0.6 ± 2.5	5.2 ± 4.6	
AREQ	3.4 ± 1.8	22.4 ± 1.8	SNAPP
AREQ	3.3 ± 0.2	10.3 ± 0.3	CAP
difference	0.1 ± 1.9	12.1 ± 1.8	
MeanBias	-0.8 ± 1.1	8.9 ± 1.9	SNAPP-CAP

All uncertainties in this table (and in the text) are one sigma standard errors.

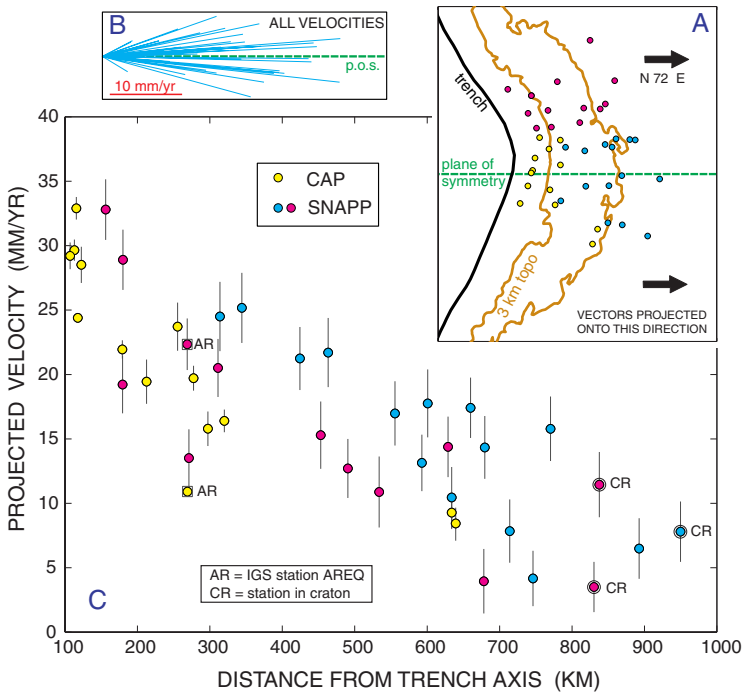

Figure 4. *Comparison of interseismic velocity solutions produced by CAP and by SNAPP [Norabuena et al., 1998] for stations located over the 'steep slab' section of the central Andes. The GPS velocity vectors are transformed into the oblique spherical coordinate system (α, β) of* Gephardt [1994] *in which the 'equator' ($\alpha = 0°$) coincides with the surface trace of the vertical plane of maximum bilateral topographical symmetry between the north and south limbs of the Bolivian Orocline. This plane, the trench axis, and the 3-km elevation contour are shown in* ***Figure 4a*** *along with all relevant GPS stations. CAP stations are yellow, and SNAPP stations are blue or magenta depending on their location. All transformed velocity vectors are stacked in* ***Figure 4b*** *so as to emphasize their directional distribution relative to the plane of topographic symmetry.* ***Figure 4c*** *shows a velocity profile for each group of stations. Each profile shows the β or 'longitudinal' component of velocity versus the distance between the trench axis and the GPS station measured along a line of 'latitude'. In effect, both velocities and distances are projected onto the direction N72°E. The blue SNAPP stations are located immediately 'downstream' of the CAP stations. However, these two profiles are not contiguous near the overlap distance of 300–330 km. Instead, the SNAPP stations are moving ~10 mm/yr faster than the CAP stations, suggesting that SNAPP's nominally craton-fixed frame is moving at about this rate relative to CAP's craton-fixed frame, at least near the boundary between the yellow and blue sets of stations. Note that the discrepancy between the two solutions for IGS station AREQ is of similar magnitude. Note also that three SNAPP stations located just east of the deformation front (within the craton) have an average (projected) velocity of ~7.5 mm/yr.*

hand, when a reference frame is defined and realized on the basis of a small number of stations whose velocities are not well resolved, the reference frame may also be poorly resolved. We suggest that this can explain much of the velocity bias in the SNAPP results.

[15] *Norabuena et al.* [1998] classified only two of their rover stations (RBLT and SJCH) as cratonic. We believe that SNAPP rover stations PSUC (Figure 3), FITZ (Figure 2) and REYE (Figure 2) are also located in the craton. Note their positions relative to our best estimate of the active deformation front (the magenta curve in Figures 2 and 3, modified from *Jordan et al.* [1983]). The mean velocity of these three stations (in the SNAPP solution) has north and east components of +1.7 mm/yr and +7.4 mm/yr, respectively. We present elsewhere a model for elastic loading of the upper plate associated with coupling across the main plate boundary which suggests that

interseismic deformation within this portion of the plate boundary should amount to 1 – 2 mm/yr. This suggests that this suite of cratonic stations is moving about 6 mm/yr too fast in an eastward direction. This is less than we might expect on the basis of our previous analysis. Furthermore, SNAPP's stations RBLT and SJCH, which are located further into the craton, have an average westward motion of 1.6 mm/yr. This suggests that it may not be possible to account for the velocity bias between the CAP and SNAPP velocity fields purely in terms of a simple reference frame problem in which one frame is moving rigidly relative to the other.

5. Tectonic Implications of the GPS Results

[16] It would be premature to attempt a detailed interpretation of the composite velocity field (Figure 3). The apparent velocity gradients near the boundaries between the SNAPP and CAP networks are almost certainly spurious. Nevertheless, we can discuss our own results, and with caution, we can compare trends internal to each network solution.

[17] CAP station YAVI and its neighbor to the south, which lie just west of the sub-Andean belt, have similar velocities (Figure 3). Their mean velocity is 8.9 ± 1.6 mm/yr bearing N70°E. Geological studies indicate that the thin-skinned fold and thrust belt has been shortened by 210–370 km in the last 27 Myr [*Sheffels*, 1990; *Gubbels et al.*, 1993; *Schmitz*, 1994], implying an average convergence rate of 8–14 mm/yr. The agreement between the geological estimates and our initial geodetic result is encouraging.

[18] The mean direction of the CAP GPS vectors (Figure 3) is N69°E. In this latitude range the mean azimuth of Nazca-South America (Nazca–SoAm) convergence is about N78°–79°E according to NUVEL [*DeMets et al.*, 1990, 1994] and *Angermann et al.* [1999]. Since the GPS average mostly reflects motion of the forearc, this difference could be accounted for by backarc convergence being oblique to Nazca-SoAm convergence. It is intriguing that CAP's mean GPS azimuth lies close to that (N72°E) of Gephart's *[Gephart*, 1994] plane of maximum bilateral symmetry (Figure 4a). It is too soon to draw any firm conclusions about this coincidence, both because there are serious disagreements between the published estimates for the Nazca-SoAm Euler vector [*DeMets et al.*, 1990, 1994; *Larson et al.*, 1997; *Norabuena et al.*, 1998; *Angermann et al.*, 1999] and because there is no formal statement of uncertainty for the azimuth of Gephart's symmetry plane.

[19] Although the coastline deflects very sharply at Arica, the change in the orientation of the trench and the plate boundary is much more gentle (Figures 2 and 3). While there is no present concensus about the precise direction of Nazca-SoAm convergence near Arica, there is no doubt that this direction can change very little between about 16°S and 22°S. A major change in the obliquity of subduction therefore takes place between AREQ and the southernmost coastal CAP station in Figure 3. However, there is no clear and significant rotation of the CAP velocity vectors in this latitude range. (The same is true of the SNAPP vectors.) This argues against major partitioning of the Nazca-SoAm plate convergence in the forearc by obliquity-driven translation of forearc slivers, as observed, for example, in Sumatra [*Prawirodirdjo et al.*, 1997]. This conclusion was reached on different grounds by *Klotz et al.* [1999] in their study of the coseismic displacement field of the 1995 Antofagasta earthquake (which begins just south of the southernmost CAP stations in Figure 3). Their geodetic solution for this earthquake indicates that Nazca-SoAm plate convergence is accommodated by oblique earthquake slip with no slip partitioning. This implies that the Atacama fault system is inactive, or very nearly so.

[20] There is no obvious indication in the CAP velocity field of local block rotations within the forearc of northern Chile. Given that purely elastic effects dominate this velocity field and that our error ellipses are still quite large, it may too early to resolve small and localized anelastic

deformations within the forearc.

6. Discussion

[21] The difficulties we have experienced in relating SNAPP's velocity field to our own indicates the importance of neighboring projects actively seeking strong ties through the sharing of observations and stations. Both projects are placing a high priority on establishing stronger ties between our networks. The ties between CAP's network and the largely overlapping German network South American Geodynamic Activities (SAGA) [*Angermann et al.*, 1999; *Klotz et al.*, 1996, 1999] are fairly good and steadily improving. There can be little doubt that better integrating the velocity field north and south of the Arica deflection will lead to interesting insights into the contemporary geodynamics of the central Andes. Fortunately, the rapidly growing numbers of CGPS stations within South America, both in the craton and in the Andes, will promote stabler and more consistent regional reference frames. This circumstance, and the inevitable passing of time since our first (baseline) measurements were made, will lead to much improved velocity solutions in the next 2 or 3 years.

Table 2. CAP Velocity Solutions.

Station	Longitude	Latitude	v_E	v_N	σ_{v_E}	σ_{v_N}	N-E Corr	Type
Cratonic South American Reference Stations								
BRAZ	-47.8779	-15.9475	-0.13	0.51	0.95	0.47	-0.010	CGPS
FORT	-38.4256	-3.8774	-0.94	1.03	0.63	0.19	0.081	CGPS
KOUR	-52.8060	5.2522	1.52	-0.03	0.63	0.24	0.004	CGPS
LHCL	-65.5952	-38.0027	-0.57	-0.05	0.73	0.83	-0.154	CGPS
LPGS	-57.9323	-34.9067	-1.66	-0.62	0.40	0.37	-0.060	CGPS
PARA	-49.2310	-25.4484	0.65	-1.08	1.98	1.35	0.075	CGPS
PARC	-70.8799	-53.1370	1.29	0.13	0.86	0.90	0.033	CGPS
UEPP	-51.4085	-22.1199	0.90	-1.19	2.24	1.52	0.059	CGPS
Other South American Reference Stations								
ANTC	-71.5321	-37.3387	14.98	-0.97	0.48	0.59	-0.183	CGPS
AREQ	-71.4928	-16.4655	10.29	3.26	0.25	0.17	-0.188	CGPS
CFAG	-68.2326	-31.6022	6.92	1.04	0.31	0.33	-0.211	CGPS
COPO	-70.3382	-27.3845	21.20	6.81	0.31	0.32	-0.240	CGPS
COYQ	-71.8921	-45.5143	-3.14	0.46	2.26	2.37	-0.043	CGPS
IQQE	-70.1317	-20.2735	23.89	5.43	0.44	0.40	-0.230	CGPS
SANT	-70.6686	-33.1503	18.42	4.33	0.19	0.29	-0.299	CGPS
TUCU	-65.2304	-26.8433	1.63	-0.18	0.43	0.38	-0.237	CGPS
Other Reference Stations								
ASC1	-14.4121	-7.9512	-5.45	-0.44	1.85	0.97	0.051	CGPS
EISL	-109.3833	-27.1482	65.21	-15.04	0.62	0.51	0.106	CGPS
Rover Stations								
ANCQ	-68.7206	-19.5266	18.06	8.14	1.17	1.45	-0.051	RGPS
ARIC	-70.3321	-18.4807	20.45	8.08	1.16	1.01	-0.138	RGPS
CHNG	-69.1678	-18.2627	13.25	10.22	1.56	2.01	-0.075	RGPS
PBLN	-70.2301	-22.1730	27.21	10.78	2.06	1.52	0.049	RGPS
PPST	-68.8349	-20.9751	23.24	5.27	2.58	2.22	-0.805	RGPS
PSAG	-70.2196	-19.6023	27.22	8.50	1.68	2.12	-0.051	RGPS
PTCH	-70.1179	-21.1460	30.54	12.50	1.86	1.20	-0.061	RGPS
SCNA	-69.6185	-18.9079	17.52	8.98	2.08	2.30	-0.523	RGPS
SLAS	-68.2777	-21.6525	15.13	6.44	2.97	1.22	0.232	RGPS
TRES	-65.4755	-22.9798	7.67	3.63	2.25	1.80	0.009	RGPS
VRDS	-70.1645	-20.4270	27.79	10.44	2.31	0.96	-0.134	RGPS
YAVI	-65.4892	-22.1379	8.98	2.45	2.33	1.62	-0.320	RGPS

The table specifies station code (Station), longitude and latitude in degrees, the east (v_E) and north (v_N) components of velocity, one sigma standard errors for these velocity components (σ_{v_E} and σ_{v_N}), the correlation coefficient for the north and east components of velocity (N-E Corr), and the station type (Continuous GPS or Rover GPS).

Acknowledgments

[22] This research was funded by the National Science Foundation. Additional support was provided by the Instituto Geográfico Militar de Chile and the Instituto Geográfico Militar de Argentina. The Instituto Brasileiro de Geografia e Estatística kindly provided us with data from their CGPS stations PARA and UEPP. We thank Rick Allmendinger, Bryan Isacks, Ben Brooks, and Robert Reilinger for informal reviews of an earlier manuscript. We thank Juergen Klotz and Detlef Angermann for many useful discussions and for their comradeship in the field. We deeply appreciate the willingness of Yehuda Bock, Peng Fang, and Robert King to provide us with technical advice whenever we have requested it. Reviews by John Beavan and Simon Lamb led to improvements in this presentation, and we thank them too. This is SOEST contibution 4894 and CERI contibution 394.

Appendix

[23] All CAP velocity solutions used in this paper are listed in Table 2. (The solutions published by *Norabuena et al*. [1998] are tabulated on the Webpage www.sciencemag.org/feature/data/975403.shl)

References

Allmendinger, R., T. Jordan, S. Kay, and B. Isacks, The evolution of the Altiplano–Puna Plateau of the central Andes, *Ann. Rev. Earth Planet. Sci., 25*, 139–174, 1997.

Angermann, D., J. Klotz, and C. Reigber, Space-geodetic estimation of the Nazca–South America Euler vector, *Earth Planet. Sci. Lett., 171*, 329–334, 1999.

Barazangi, M., and B. Isacks, Spatial distribution of earthquakes and subduction of the Nazca plate beneath South America, *Geology, 4*, 686–692, 1976.

Beck, M., Analysis of Late Jurassic–Recent paleomagnetic data from active plate margins of South America, *J. S. Am. Earth Sci., 1*, 39–52, 1988.

Beck, M., On the mechanism of crustal block rotations in the central Andes, *Tectonophysics, 299*, 75–92, 1998.

Bevis, M., and B. L. Isacks, Hypocentral trend surface analysis: Probing the geometry of Benioff zones, *J. Geophys. Res., 89*, 6153–6170, 1984.

Bevis, M., Y. Bock, P. Fang, R. Reilinger, T. Herring, J. Stowell, and R. Smalley, Blending old and new approaches to regional geodesy, *Eos Trans. AGU, 78*, 61, 64, 66, 1997.

Cahill, T., and B. L. Isacks, Seismicity and shape of the subducted Nazca plate, *J. Geophys. Res., 97*, 17,503–17,529, 1992.

DeMets, C., R. G. Gordon, F. Argus, and S. Stein, Current plate motions, *Geophys. J. Int., 101*, 425–478, 1990.

DeMets, C., R. G. Gordon, F. Argus, and S. Stein, Effect of recent revisions of the geomagnetic timescale on estimates of current plate motions, *Geophys. Res. Lett., 21*, 2191–2194, 1994.

Engdahl, E.R., R. D. Van der Hilst, and R. P. Buland, Global teleseismic earthquake relocation with improved travel times and procedures for depth determination, *Bull. Seismol. Soc. Am., 88*, 722–743, 1998.

Gelb, A., *Applied Optimal Estimation*, 374 pp., MIT Press, Cambridge, Mass., 1974.

Gephart, J., Topography and subduction geometry in the central Andes: Clues to the mechanics of a noncollisional orogen, *J. Geophys. Res., 99*, 12,279–12,288, 1994.

Gubbels, T., B. Isacks, and E. Farrar, High-level surfaces, plateau uplift, and foreland development, Bolivian central Andes, *Geology, 21*, 695–698, 1993.

Isacks, B., Uplift of the central Andean plateau and bending of the Bolivian Orocline, J. Geophys. Res., 93, 3211–3231, 1988.

Jordan, T., B. Isacks, R. Allmendigner, J. Brewer, V. Ramos, and C. Ando, Andean tectonics related to geometry of the subducted Nazca plate, *Geol. Soc. Am. Bull., 94*, 341–361, 1983.

Kendrick, E., M. Bevis, R. Smalley, O. Cifuentes, and F. Galban, Current rates of convergence across the central Andes: Estimates from continuous GPS observations, *Geophys. Res. Lett., 26*, 541–544, 1999.

Klotz, J., J. Reinking, and D. Angermann, Die vermessung der deformation der erdoberflaeche, *Geowissenschaften, 14*, 389–394, 1996.

Klotz, J., D. Angermann, G. Michel, R. Porth, C. Reigber, J. Reinking, J. Viramonte, R. Perdomo, V. Rios, S. Barrientos, R. Barriga, and O. Cifuentes, GPS-derived deformation of the central Andes including the 1995 Antofagasta $M_w = 8.0$ earthquake, *Pure Appl. Geophys., 154*, 709–730, 1999.

Larson, K., J. Freymueller, and S. Philipsen, Global plate velocities from the Global Positioning *System, J. Geophys. Res., 102*, 9961–9981, 1997.

Leffler, L., S. Stein, A. Mao, T. Dixon, M. Ellis, L. Ocola, and S. Sacks, Constraints on present-day shortneing rate across the central eastern Andes from GPS data, *Geophys. Res. Lett., 24*, 1031–1034, 1997.

McCaffrey, R., Global variability in subduction thrust zone–forearc systems, *Pure Appl. Geophys., 142*, 173–224, 1994.

Norabuena, E., L. Leffler-Griffin, A. Mao, T. Dixon, S. Stein, I. Sacks, L. Ocala, and M. Ellis, Space geodetic observation of Nazca–South America convergence across the central Andes, *Science, 279*, 358–362, 1998.

Nur, A., and Z. Ben Avraham, Volcanic gaps and the consumption of aseismic ridges in South *America, Mem. Geol. Soc. Am., 154*, 729–740, 1981.

Pilger, R., Plate reconstructions, aseismic ridges and low angle subduction beneath the Andes, J. *Geol. Soc. London, 141*, 793–802, 1981.

Prawirodirdjo, L., Y. Bock, R. McCaffrey, J. Genrich, E. Calais, C. Stevens, S. Puntodewo, C. Subarya, J. Rais, P. Zwick, and Fauzi, Geodetic observations of interseismic strain segmentation at the Sumatran subduction zone, *Geophys. Res. Lett., 24*, 2601 –2604, 1997.

Randall, D., A new Jurassic–Recent apparent polar wander path for South America and a review of central Andean tectonic models, *Tectonophysics, 299*, 49–74, 1998.

Sheffels, B., Lower bound on the amount of crustal shortening in the central Bolivian Andes, *Geology, 18*, 812–815, 1990.

Schmitz, M., A balanced model of the southern central Andes, *Tectonics, 13*, 484–492, 1994.

Von Huene, R., J. Corvalán, E. Fluch, K. Hinz, J. Korstgard, C. Ranero, W. Weinrebe, and the CONDOR Scientists, Tectonic control of the subducting Juan Fernández Ridge on the Andean margin near Valparaiso, Chile, *Tectonics, 16*, 474–488, 1997.

Zhang, J., Y. Bock, H. Johnson, P. Fang, S. Williams, J. Genrich, S. Wdowinski, and J. Behr, Southern California Permanent GPS Geodetic Array: Error analysis of daily position estimates and site velocities, *J. Geophys. Res., 102*, 18,035–18,055, 1997.